



# Design and Optimization of Solar Powered Irrigation System using Artificial Intelligent Techniques

Santosh Singh Raghuwanshi\*, Safdar Sardar Khan and Ratnesh Litoriya

Department of Computer Science and Engineering, Medicaps University, Indore, MP, India

Received: 30.10.2024 Accepted: 21.03.2025 Published: 30.03.2025

\*santoshraghuwanshi@gmail.com



## ABSTRACT

The main objective of this study is the design and optimization of a solar photovoltaic (PV) powered irrigation system using artificial intelligence (AI) techniques. To employ AI approaches, including fuzzy logic, particle swarm optimization (PSO), artificial neural networks (ANN), and machine learning (support vector machine (SVM)), as controllers in maximum power point tracking (MPPT) systems to optimize PV systems. These techniques are also employed to regulate speed and torque in a moto-pump system. PV power generation has been predicted using the ML approach. The results indicate that the machine learning-based photovoltaic system achieves maximum power under varying weather conditions. At a reference speed of 300, the average speeds of Fuzzy, PSO, ANN, and ML are 292.3 rad/sec, 294.6 rad/sec, 298.4 rad/sec, and 300 rad/sec, respectively. In terms of overshoot and settling time, ML performs better. The ML-based system has 99.6% efficiency and is continuously maintained. The ML technique improves the performance of PV systems compared to the PSO, fuzzy, and ANN techniques. This work is highly beneficial for government agencies and stakeholders involved in irrigation systems.

**Keywords:** ANN; PV system; Machine learning; PSO; Support vector machine.

## 1. INTRODUCTION

Solar radiation produces approximately a billion kWh of energy annually, which can be converted into heat and electricity with an efficiency of 10 to 25%. Solar PV cells convert sunlight into electricity, and their production has increased by over 40% annually since 2020, making them a rapidly growing energy technology. The agriculture industry in India consumes approximately 17-26% of total electricity (Koç, 2018). The implementation of a solar PV water pumping system (SPVWPS) is an optimal solution for irrigation in developing countries. These pumps convert solar energy into electricity, running a set of motor pumps compatible with a solar array. They are commonly used in wells, borewells, ponds, and canals. According to the PM-KUSUM plan, a total of 2,18,539 solar pumps have been successfully implemented in agricultural areas across India as of March 31, 2023. The current cost to farmers to install a solar pump under the initiative is approximately Rs. 1.5 lakhs. The main drawbacks of SPVWPS are its high cost and low efficiency, ranging from 8% to 18%. AI technology has wholly changed the agricultural industry. AI plays a vital role in improving SPVWPS performance. In India, SPVWPS is offering an environmentally responsible and sustainable water delivery system. Numerous advantages have resulted from the incorporation of AI technology with SPVWPS, including reduced costs, enhanced dependability, streamlined operation, and improved efficiency

(Mohammad and Mahjabeen, 2023). The MPPT method plays a vital role in improving the performance of SPVWPS by ensuring that the PV panels run at their maximum power output. The integration of AI technology with the MPPT system enhances the efficiency of SPVWPS (Venkat *et al.* 2024).

Mahesh *et al.* (2022a) introduces a machine-learning algorithm for MPPT in isolated PV systems. The algorithm uses a decision tree regression strategy to predict the maximum power available as well as the module voltage for specific irradiance and temperature. Simulations show that the suggested method increases efficiency by over 93.9% in a steady state. This indicates that machine learning techniques can be used to control nonlinear energy production in PV systems. Ahmed *et al.* (2022) presents a deep learning model using a back-propagation neural network (BPNN) to maximize the power output of the solar grid under various load conditions. The model predicts the reference voltage and ensures a stable output voltage. The model is tested under different conditions, achieving maximum output power with 98% accuracy compared to existing methods. Meena *et al.* (2022) explore AI methods for scaling solar power systems, including standalone, grid-connected, and hybrid systems, to reduce environmental impact. It proposes a new model using multilayered perceptrons, which works with current PV modules. The performance is evaluated based on the convergence speed for single, two, and three diodes. Sharmin *et al.* (2022) present an

automated calibration approach for maximum power point tracking algorithms in solar PV systems. The method employs a simplified drawing of a PV system and an improved neural network (NN) method to monitor the maximum power point (MPP) of solar cell modules. The Bayesian regularisation approach is selected for training, and theoretical findings indicate that the enhanced neural network MPPT algorithm exhibits superior efficiency relative to the perturb and observe (P&O) method, minimizing misjudgment and power loss around the MPP. Khan *et al.* (2023) offer a neural network-based MPPT control approach for hybrid PV systems. The snake optimiser changes the multilayer perceptron neural network (MLPNN) weights and biases to make it faster and better at monitoring global maxima in real time. The PID controller that uses the snake optimizer, in conjunction with the snake optimizer-based neural network (SOANN), delivers stability, precision, and rapid MPPT under diverse environmental circumstances. The SOANN controller surpasses conventional controllers for efficiency, tracking time, stability, and fault detection capability in diverse practical conditions.

Mahesh *et al.* (2022a) presents regression machine learning algorithms to extract maximum power from an isolated PV panel. Linear and non-linear algorithms predict available power and voltage, determining the duty cycle for a boost converter. The method achieves a steady state MPPT efficiency of over 95.21%, with better accuracy under variable climatic conditions compared to existing methods. (Kirubakaran and Singaravelu, 2024) introduce an ML-based Support Vector Regression (SVR) MPPT controller, which they benchmark against AI-based methods. The SVR algorithm detects the maximum power and voltage, enabling an energy-efficient system. The proposed SVR algorithm offers better stability and operates at 96.60% of the mean efficiency, regardless of climatic changes. (Agarwal *et al.* 2022) presents a data-driven ML algorithm to track maximum power in PV panel systems. The algorithm uses data from the panel system connected to a boost converter, predicting PV voltage, current, temperature, irradiance, and PI. The system becomes more efficient (98%) over time. The system uses ensemble-based machine learning models to estimate power production from six solar PV systems, demonstrating strong performance and low computing costs. These models surpass the k-nearest neighbor method for real-time PV performance prediction (Raj *et al.*, 2023).

Ourici and Abderaouf, (2023) Compare the effectiveness of an ANN in monitoring MPP in PV systems with the traditional P&O technique. The NN was trained using data from a 100 Kw PV system, including performance measurements and environmental conditions. With a response time of 0.156 s, the NN method was faster, reaching a maximum power of 100 kw. Omer and Shareef, (2023) introduce a machine-

learning gradient boost controller for PV systems using the CatBoost methodology. This controller outperforms conventional PI controllers in a variety of load, irradiance, and partial shade scenarios. Bacanin *et al.* (2023) present an AI-based energy predict-tuned deep learning framework for renewable energy sources (RES), which addresses hyperparameter tuning for long short-term memory (LSTM) and gated recurrent unit (GRU) neural networks. Li *et al.* (2023) discusses the integration of AI, big data, and energy management systems, focussing on their role in forecasting energy use, facilitating energy trading, and transitioning to a lower carbon system. Habib *et al.* (2023) presents an SPVWPS designed to meet the growing global demand for water. The system considers water requirements, solar resources, tilt angle, losses, and performance ratio. The PV system, installed at a 15° tilt angle, is more efficient than diesel engines. The system pumps 75054 m<sup>3</sup> of water, supplying 92.9% of the irrigation demand. The system has an annual average performance ratio of 74.6%, and 70.0% of farmers are extremely satisfied with it.

Pandian *et al.* (2024) suggest a real-time defect detection method for solar PV systems that uses a hybrid ANN and SVM. This method improves performance by combining the benefits of both algorithms to find faults faster and more accurately. Using ultra-short-term PV power forecasts, Mingzhang (Pan *et al.* 2020) optimized grid-connected solar power. Data pretreatment techniques build an SVM, leading to a 6.8% increase in the regression coefficient (R<sup>2</sup>). The hybrid model has an R<sup>2</sup> of 0.997, enhancing forecast accuracy for peak power and night, thus improving real-time grid-connected generation capabilities. Der *et al.* (2024) proposed a method to enhance fault detection in solar power systems by analyzing common defect types in PV modules and using SVM techniques. They used data analysis to identify system errors and create an interface for real-world monitoring. The system accurately identified eight main problems, including energy storage batteries, solar panel output circuits, dust buildup, inverters, controllers, and damage to the mounting rack structure. The approach also detects open-circuit and short-circuit defects in bypass diodes. The above study reviews the AI applications in renewable energy systems, focussing on modeling techniques for solar power forecasting, fault detection, and intelligent buildings. AI can also improve the design, modelling, optimisation, control, and efficiency of renewable energy systems. This work is focused on these research gaps. The novelties of this work are:

1. The solar PV energy system is designed to meet the daily water demand.
2. To use AI (PSO, fuzzy, ANN, and ML) techniques to enhance and analyze MPPT performance under various weather scenarios.

3. To use AI approaches to control the motor pump system speed and torque.
4. Use the ML (SVM) technique to anticipate and compare the actual generation of PV electricity.
5. To compare the performance of ML (SVM) approaches to that of fuzzy, PSO, and ANN techniques.

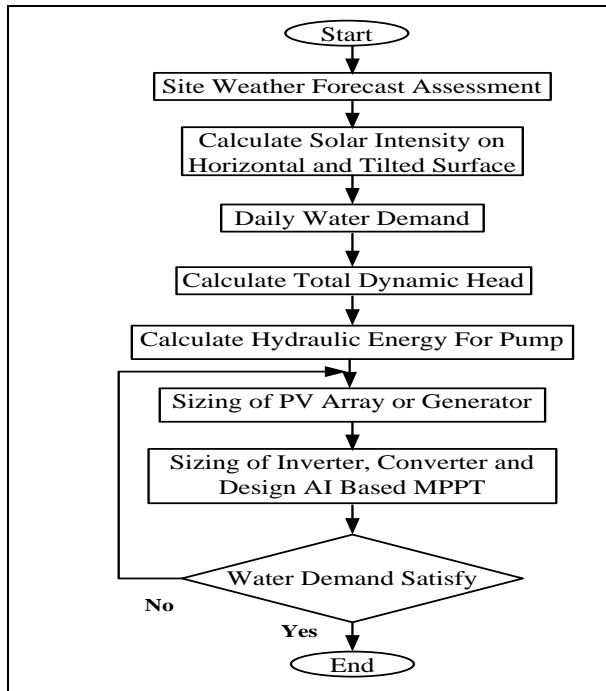


Fig. 1: Flow chart of the design and sizing of SPIS

## 2. DESIGN METHODOLOGY

The mathematical design methodology of the solar power irrigation system (SPIS) is illustrated in Figure 1. A 5-acre farm is being considered for this investigation. The farmhouse is situated at a latitude of 24.34 N and a longitude of 77.43 E. The 5-acre farm accommodates a family of six members, consisting of three males and three females, as well as animals that require drinking water for both the family and the animals themselves. The farm also needs water every day for farming reasons. The daily water demand in the farmhouse is 30,000 liters. The depth of the well is 70 meters.

To calculate the sizing of the PV system as follows:

Step 1: Assessment of site weather forecast using AI techniques. The yearly average solar radiation intensity is shown in Figure 1.

Step 2: Determine the solar energy received on a horizontal surface. The horizontal surface is calculated by equation 1.

$$H_s = \frac{86400 G_c}{\pi} \left(1 + 0.33 \cos\left(2\pi \frac{n}{365}\right)\right) (\cos\phi \cos\delta \sin\omega_s + \omega_s \sin\phi \sin\delta) \quad \dots (1)$$

Where  $G_c$  and  $n$  are the solar constant and No. of days, respectively,  $\omega_s, \phi, \delta$  are the sunset hour, latitude, and declination angle.

Step 3: Calculate the daily water demand. The daily water demand is 30,000 liters/day.

Step 4: Compute the total dynamic head (TDH). The TDH is (Raghuwanshi and Khare, 2018),

$$\text{TDH} = \text{Vertical head} + \text{Frictional losses (0.5\%)} = 73.5 \text{ meters} \quad \dots (2)$$

Step 5: Determine the daily hydraulic energy need. The hydraulic energy is (Raghuwanshi and Khare, 2018),

$$E_{hy} = \frac{(\rho \times v \times g \times \text{TDH} \times 10^{-3} \text{ MJ})}{3.6} = 6 \text{ kWh} \quad \dots (3)$$

Where,  $\rho, v$  and  $g$  are the density of water (1000 kg/m<sup>3</sup>), gravity (9.81 m/s<sup>2</sup>) and volume of water (30,000 litres/day) respectively.

Step 6: Size of the PV capacity (kW) needed to power the pump's electric load (Raghuwanshi and Khare, 2018).

$$P_{pv} = \frac{E_{hy}}{G_d \eta_e m_f O_f} \text{ KW} = 4.48 \text{ kW} \approx 5 \text{ kW} \quad \dots (4)$$

Where,  $G_d$  and  $\eta_e$  are the daily solar irradiation on PV surface in kwh/m<sup>2</sup> (6h/day) and subsystem efficiency (0.35) respectively.  $m_f$  and  $O_f$  are the mismatch (0.85) and operating (0.75) factors, respectively.

Step 7: Calculate motor pump, inverter, and converter ratings.

A 3 ph/3.7 kW submersible pump is used. The efficiency of solar inverter and converter are usually, 93-96%. The inverter rating is (Raghuwanshi *et al.* 2023),

$$P_{inv} = \frac{3.7 \text{ kW}}{0.95} = 3.89 \approx 4 \text{ kW} \quad \dots (5)$$

The DC-DC converter rating is (Raghuwanshi *et al.* 2023),

$$P_{con} = \frac{4 \text{ kW}}{0.93} = 4.30 \approx 4.5 \text{ kW} \quad \dots (6)$$

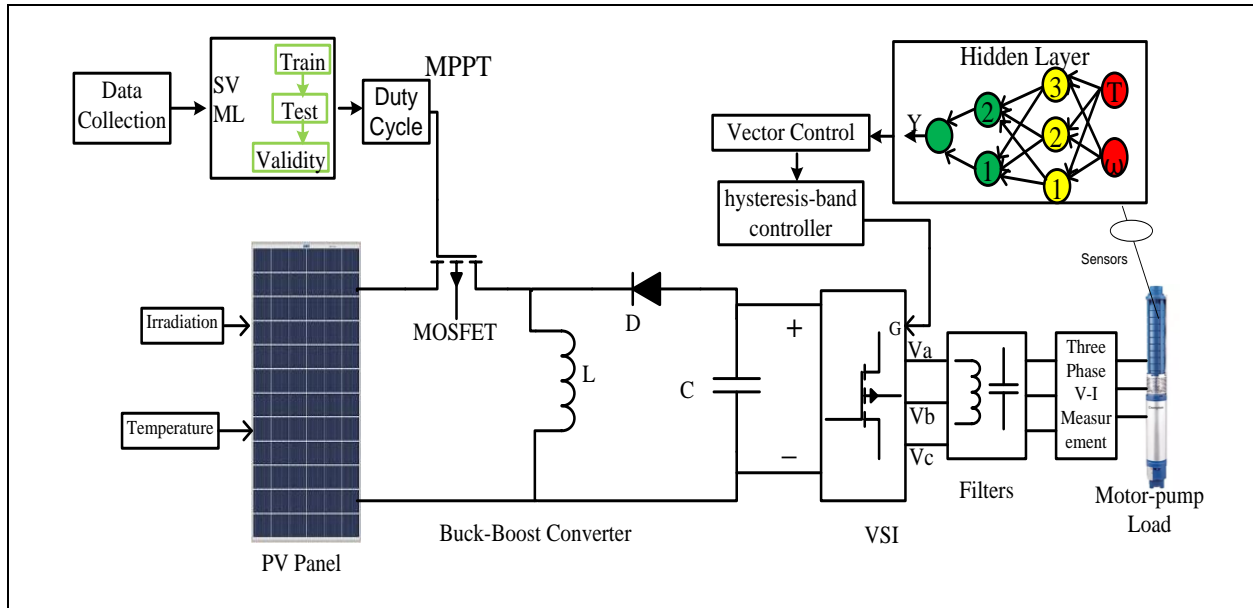


Fig. 2: AI-based solar PV water pumping system

### 3. SYSTEM DESCRIPTION

The SPIS comprises a PV module, a DC-DC converter (buck-boost), a voltage source inverter (VSI), filters, and a motor pump and load demand. The system components are arranged in series as illustrated in Figure 2. Two control mechanisms have been used to achieve optimization. Control the MPPT first, and then use the vector control method to manage the speed of the motor pump to meet the daily water demand.

#### 3.1 PV panel

A PV cell transforms solar energy into direct current electrical energy via the photoelectric effect. A PV array consists of parallel and series PV cells, with series and shunt resistances that affect cell efficiency.

The PV generator power is as follows (Verma *et al.* 2024),

$$p_v = P_{rat} \times \frac{G_{rad}}{G_{ref}} \times [1 + k_c(T_{amb} + (0.0256 \times S_{rad})) - T_r] \dots (7)$$

Where,  $P_{rat}$  and  $k_c$  represent rated PV power and constant ( $-3.7 \times 10^{-3}$  ( $1/^\circ C$ )) respectively,  $G_{rad}$  and  $G_{ref}$  represent sun and reference irradiation respectively,  $T_{amb}$  and  $T_r$  are the ambient and reference temperature respectively.

#### 3.2 Buck-boost Converter

PV voltage is increased by the DC-DC buck-boost converter, which is driven by a PV panel and managed by PWM. It does this by utilizing the duty ratio of a metal oxide field effect transistor (MOSFET). An

inductor is used in the circuit to boost current, and when the switch is off, stored energy is released.

The output voltage is as follows,

$$V_o = -\frac{D}{1-D} V_{in} \dots (8)$$

The inductance and capacitance are as follows:

$$L = \frac{V_o D}{\Delta I f} \dots (9)$$

$$C = \frac{V_o D}{\Delta V_c f R} \dots (10)$$

Where,  $V_{in}$  and  $V_o$  represent input and output voltage respectively,  $D$  is duty cycle,  $\Delta I$  and  $\Delta V_c$  represent ripple current and voltage respectively,  $f$  and  $R$  represent switching frequency and output resistance (Abid *et al.* 2021).

$$\eta_{con} = \frac{V_o I_o}{V_{pv} I_{pv}} \dots (11)$$

#### 3.3 Inverter

A solar pump inverter is a crucial component of off-grid solar systems, converting direct current from solar panels into alternating current for powering appliances like water pumps. It maintains a constant frequency, ensuring smooth operation during electrical outages.

#### 3.4 Motor-pump Set

Solar submersible pumps utilize solar energy for water delivery, making them ideal for remote areas with

limited electricity, providing domestic, agricultural, and livestock water supply, irrigation, and borehole pumping.

#### 4. AI TECHNIQUES

Three AI approaches have been taken into consideration for solar irrigation system optimization. AI approaches such as fuzzy logic, PSO, ANN, and ML (SVM) are employed to optimize irrigation system performance.

##### 4.1 Fuzzy Logic Controller

The FLC MPPT technique is used to optimize SPIS by continuously adjusting the system operating point to align with the MPP. The technique uses fuzzy logic principles to accommodate imprecision and uncertainty, resulting in robust and efficient control. The process involves fuzzification, which transforms quantitative inputs into fuzzy language variables, and the Fuzzy Rule Base, which consists of linguistic rules derived from these variables. The Inference Engine processes these fuzzy input variables, generating fuzzy output variables and defuzzifying them into numerical values. The control actions are then transmitted to the PV inverter, which adjusts the system operation to optimize power production.

The primary variables incorporated into the FLC are the voltage error and its temporal variation. At each sample instant, two input variables,  $e(t)$  and  $\Delta e(t)$ , are computed as follows (Jayasankar *et al.* 2024),

Error,

$$e(n) = \frac{p_v(t) - p_v(t-1)}{v_v(t) - v_v(t-1)} \quad \dots (12)$$

Change of error,

$$\Delta e(t) = e(t) - e(t-1) \quad \dots (13)$$

Where,  $v_v$  and  $p_v$  are the PV voltage and power respectively.

The duty cycle of FLC is as follows (Pandey *et al.* 2024),

$$\Delta D = \frac{\sum_{i=1}^N \mu_w dD_i}{\sum_{i=1}^N \mu_w} \quad \dots (14)$$

Where,  $dD_i$  and  $\mu_w$  are the membership function and weight factor of duty cycle respectively.

The following duty cycle value is utilized to create the converter control signal:

$$D(t) = D(t-1) + \Delta D(t) \quad \dots (15)$$

##### 4.2 Particle Swarm Optimization

PSO, as a controller, can optimize power generation in solar PV systems. Regular adjustments ensure accurate control, with the PSO controller creating a population of particles for maximum power generation. The steps of the PSO algorithm are as follows,

Step 1: Initialization: initialization population of particles.

Step 2: Velocity and Position Updating: Particles adapt their velocities and positions based on MPP, ideal position, and adjacent particle positions, with factors like inertia, cognition, and social relationships influencing acceleration coefficients.

Position vectors  $p_v(t)$  and velocity vectors  $v_v(t)$  are used to classify each particle.

The velocity constraint is as follows (Sinha *et al.* 2024),

$$v_v(t+1) = \delta v_v + k_1 \times \text{ran} \times (p_{\text{best}}(t) - p_v(t)) + k_2 \times \text{ran} \times (g_{\text{best}}(t) - p_v(t)) \quad \dots (16)$$

Where,  $\delta$  and  $\text{ran}$  are the inertia weight and random numbers respectively,  $k_1$  and  $k_2$  are the cognition and social mechanisms respectively,

Step 3: Fitness Evaluation: Each particle's power output, representing the operational point, undergoes an assessment. The fitness function incorporates the positional data of the particle to determine the electrical power produced by the system.

Step 4: Updated position: The particles iteratively update both the global best position, which signifies the MPP output among all particles in the population, and their personal best positions, which denote the position with the highest power output they have encountered thus far.

The location updates of the particles by using the following equation (Gupta and Bhargava, 2024),

$$p_v(t+1) = p_v(t) + v_v(t+1) \quad \dots (17)$$

where,  $p_v(t)$  and  $p_v(t+1)$  are the position and updated vector

Step 5: Termination Criteria: The algorithm terminates its execution either when it reaches a specific number of iterations or when there is a slight marginal gain in power output.

Step 6: Control Implementation: The global best position, which represents the powerpoint with the

highest magnitude, determines the control modifications applied to the operational state of the PV system.

### 4.3 Artificial Neural Network

The ANN MPPT controller optimizes the power generation of a PV system by continuously adjusting the operating point. The ANN learns patterns and correlations from historical data, processes inputs like solar radiation, temperature, and power output, computes the maximum power point, implements control measures, and continuously monitors the optimal power point to maximize power production efficiency and performance. The goal is to maximize the PV system capabilities in dynamic operating conditions. The ANN topology of the PV system is shown in Figure 3.

The following is the activation signal of the nth hidden layer neurone (Liu *et al.* 2023),

$$a_s = \sum_{i=1}^n w_{si} V_{pv,i} I_{pv,i} + b_i \quad \dots (18)$$

Where,  $w_{si}$  and  $b_i$  are the input weight and bias vector respectively,  $V_{pv,i}$  and  $I_{pv,i}$  are the PV voltage and current input respectively.

The decision signal is calculated using the sigmoid function as follows (Liu *et al.* 2023; Bandhu *et al.* 2024),

$$S_f = \frac{1}{1+e^{-a_s}} \quad \dots (19)$$

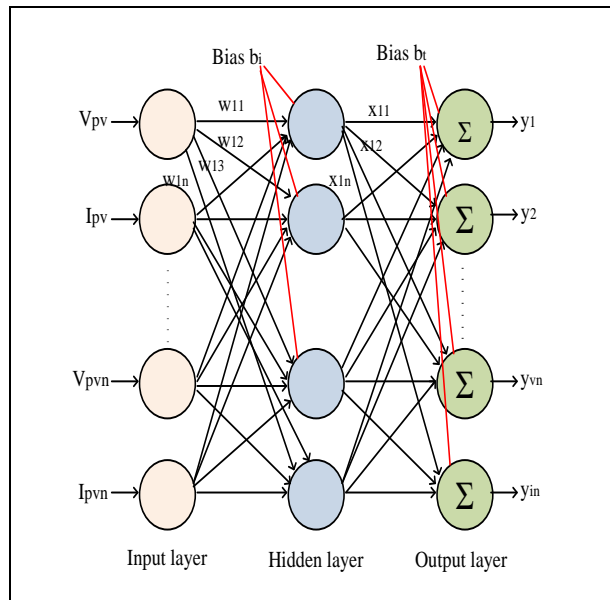


**Fig. 3: ANN for PV system**

Output can be calculated using the following equation (Bandhu *et al.* 2024; Shah *et al.* 2024)

$$y_{vin} = \sum_{j=1}^n x_{sj} S_f + b_t \quad \dots (20)$$

Where,  $x_{sj}$  and  $b_t$  are the output weight and bias vector respectively.

The study uses the normalized mean squared error as the cost function to train neural networks, aiming to minimize the cost function and improve forecast accuracy (Bandhu *et al.* 2024; Khasawneh *et al.* 2024).

$$RMSE = \frac{1}{T_m} \sqrt{\frac{1}{N} \sum_{i=1}^N (T_v - P_v)^2} \quad \dots (21)$$

Where  $T_v$  and  $P_v$  represent true and forecast values respectively,  $T_m$  and  $N$  are the mean of true value and number of data samples respectively.

### 4.4 Machine Learning Technique (Support Vector Machine)

SVM is used for classification tasks; however, it can also be modified for regression applications. It operates by determining the ideal hyperplane in a high-dimensional space to differentiate data points of various kinds. A flat affine subspace of dimension (n-1) is characterized as a hyperplane in an n-dimensional space. Figure 4 illustrates a hyperplane, which is a line in two dimensions and a plane in three. The data points closest to the hyperplane are termed support vectors, which are essential for determining the hyperplane's position and orientation. The SVM algorithm concentrates on these points to maximize the margin between the classes. The distance between the nearest data point of each class and the hyperplane is indicated by the margin. SVM enhances the model's capacity for generalization by increasing this margin.

Let us assume, training data set with  $N$  samples are denoted as  $(x_j, y_j)$ ,  $j=1,2,3,\dots,N$ . Where,  $x_j$  and  $y_j$  are represent the input and output respectively.

The linear hyperplane function is as follows (Mahesh *et al.* 2022a, Hafdaoui *et al.* 2022),

$$f(x) = \beta x + c \quad \dots (22)$$

where  $\beta$  and  $x$  are hyperplane inclination in space and a point on the plane, and  $c$  is the bias of the hyperplane from the origin.

The objective function of SVML is as follows (Pan *et al.* 2020; Deo *et al.* 2016),

$$\text{Minimize } \frac{1}{2} \|\beta\|^2 + c \sum_{j=1}^N (\xi_j - \xi_j^*) \quad \dots (23)$$

$$\text{Subject to } \begin{cases} y_j - (\beta x_j + c) \leq \epsilon + \xi_j \\ (\beta x_j + c) - y_j \leq \epsilon + \xi_j^* \end{cases} \quad \dots (24)$$

kernel function for non-linear training data is as follows,

$$f(x) = \text{sign}(\sum_{j=1}^N \beta K(x_j, x) + c) \quad \dots (25)$$

Where,  $K$  and  $x_j$  are the kernel function and support vectors respectively.

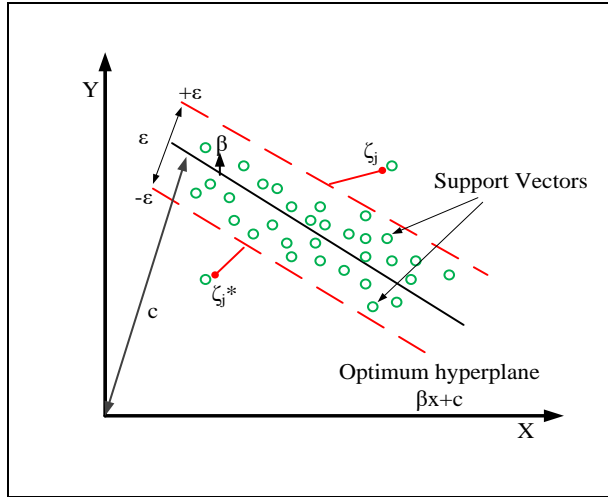


Fig. 4: SVM on two-dimensional space (Deo et al. 2016)

### 5. RESULTS AND ANALYSIS

The data for PV panels are tabulated in Table 1. Modeling of the PV module using MATLAB environment under different weather conditions is shown in Figure 5. The V-I and P-V characteristics of a solar module at 25 °C and various irradiation (300W/m<sup>2</sup>-1000W/m<sup>2</sup>) are shown in Figure 5a. For 300W/m<sup>2</sup>, the current reaches a value of around 2.85 Amp and stays constant for voltages between 0V and 33V. However, it rapidly drops with additional voltage increases and reaches zero at 36.8V. For 700W/m<sup>2</sup>, the current reaches a value of around 6.55 Amp and remains constant for voltages between 0V and 33.6V. However, it rapidly drops with additional voltage increases and reaches zero at 38.7V. The current of the PV cell reaches a value of around 9.3 amps at 1000W/m<sup>2</sup> and is constant for voltages between 0V and 39.9V. The characteristics show that as solar irradiation increases, the module voltage and current will increase.

The power output increases gradually from 0 to about 87 W at a solar irradiation level of 300 W/m<sup>2</sup>, and the voltage increases gradually from 0 V to 32.6 V. However, beyond this point, the power quickly decreases and hits zero at 37.8 V. When the solar irradiation level is 700 W/m<sup>2</sup>, and the output power gradually increases from 0 to 208 W at 33.55 V. A constant pattern in power production is seen at 1000 W/m<sup>2</sup> of solar insolation. As the voltage rises from 0 V to an ideal level, it begins at 0 W and steadily increases to about 300 W. However, beyond this, the power output quickly drops and hits 0 W at 39.9 V. These features imply that the voltage and power output of the module grow in tandem with an increase in solar insolation.

Table 1. Technical specifications of PV panel

Parameters	Specifications
Model Number	BBS24F300
Module Power	300W
Module Max. Voltage	33.90V
Maximum Current	8.85A
Open Circuit Voltage	39.90V
Short Circuit Current	9.38A
Module Sizes	164.5 cm x 99 cm x 3 cm
Efficiency	16.70%
Life Span	25 Years

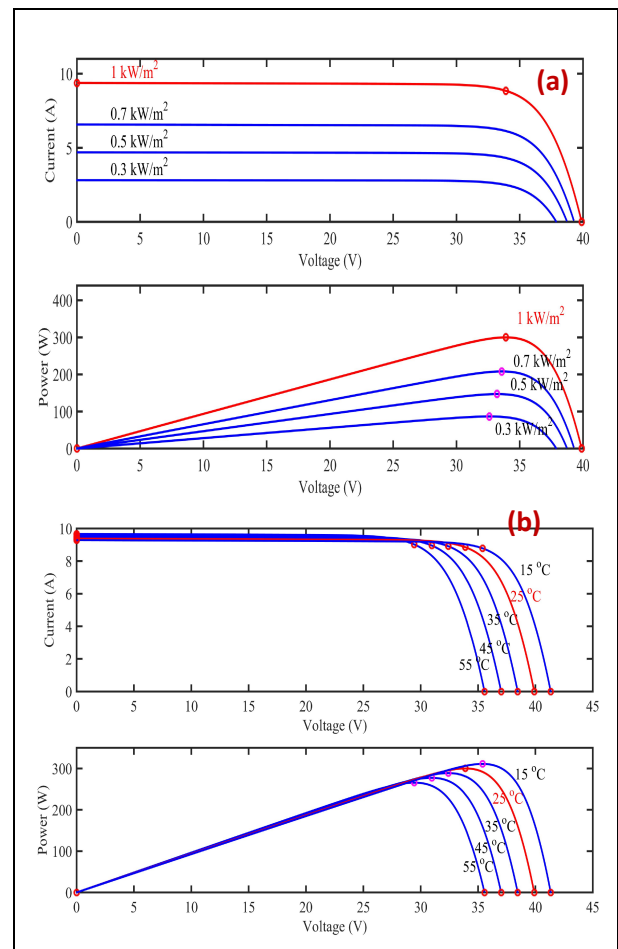


Fig. 5: I-V and P-V characteristics of PV array (a) at different solar irradiances and (b) at different temperature

Figures 5b illustrate how the I-V and PV properties of the temperature affect the solar module. When the temperature rises, the current increases slightly, but the PV cell voltage of the PV cell clearly decreases at constant insolation levels (1000W/m<sup>2</sup>). As demonstrated in Fig. 5a, a rise in temperature decreases the bandgap, increasing the rate of photogeneration. As a result, the cell current increases and the open-circuit

voltage falls. The cell voltage drops by about 2 volts and the current only increases by 0.3 A from 25 to 35 °C. It has been shown that while there is a slight rise in current,

there is a noticeable fall in voltage. It is more noticeable when the cell voltage drops than when the short-circuit current rises.

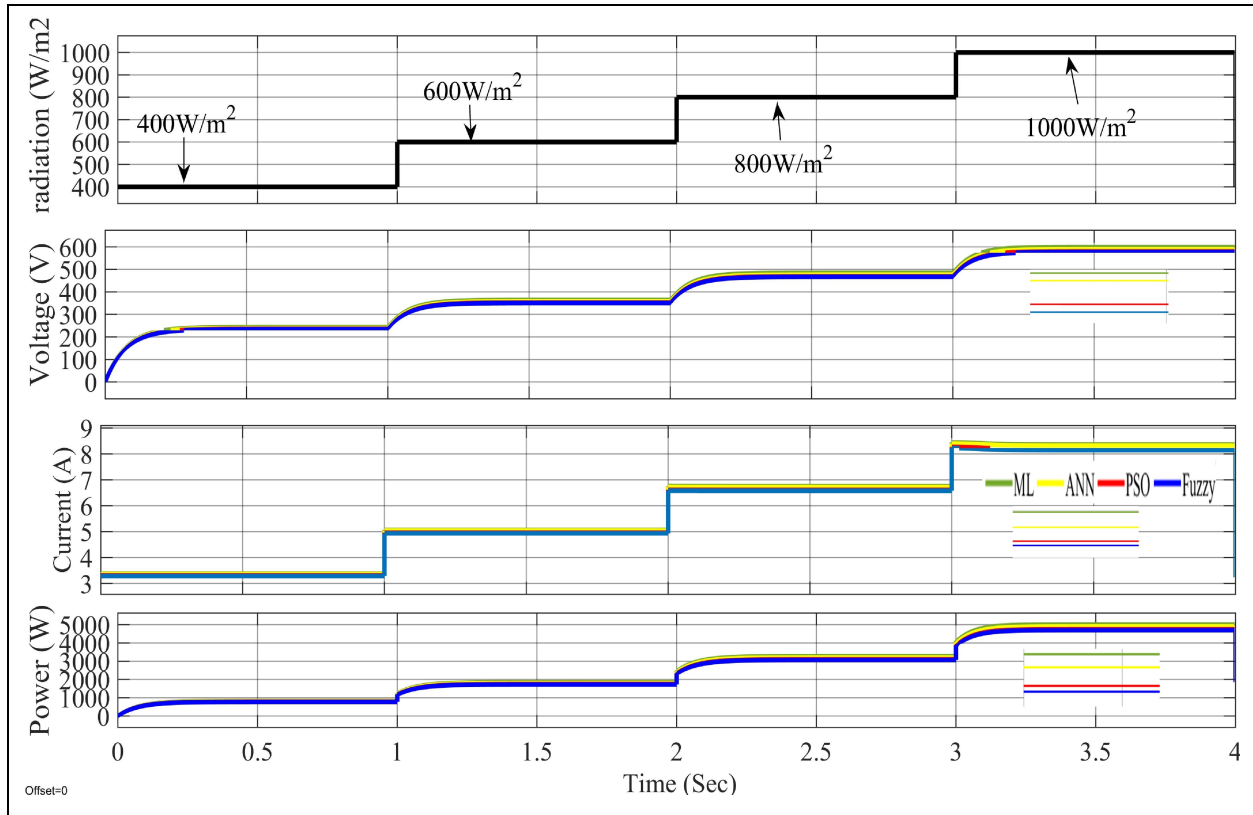
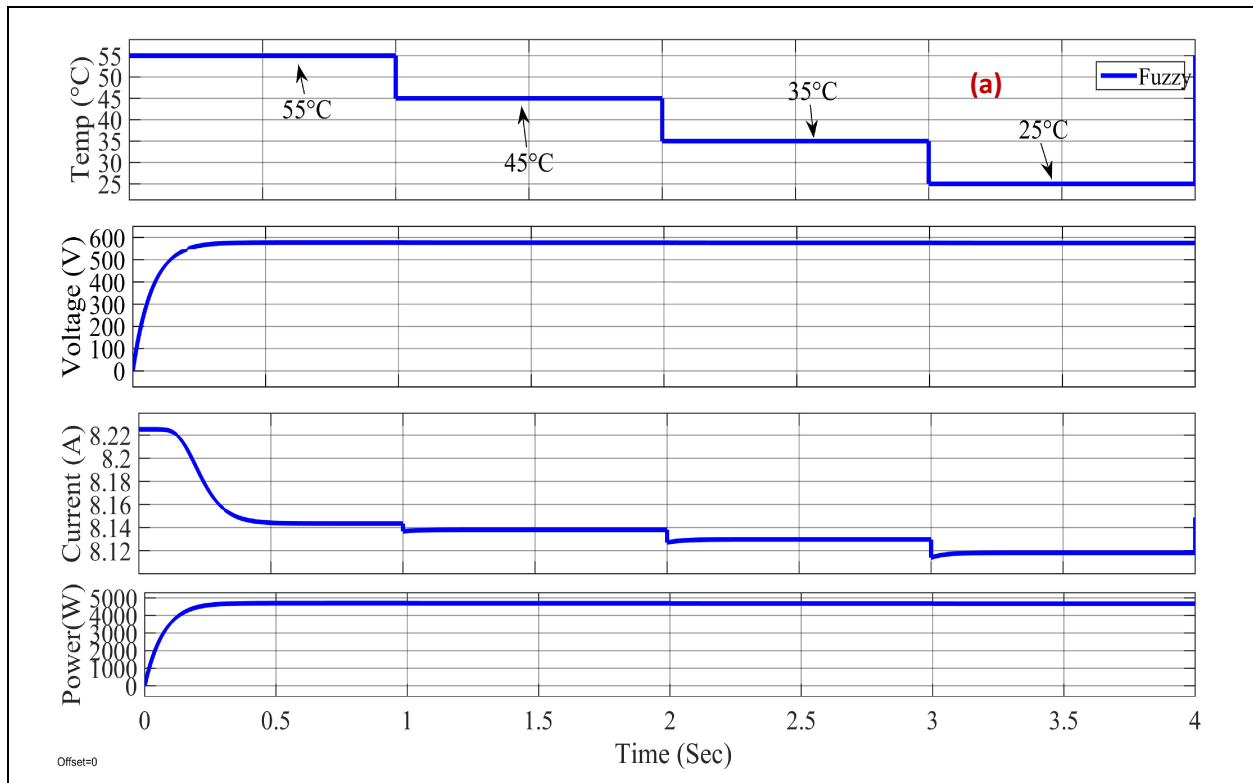
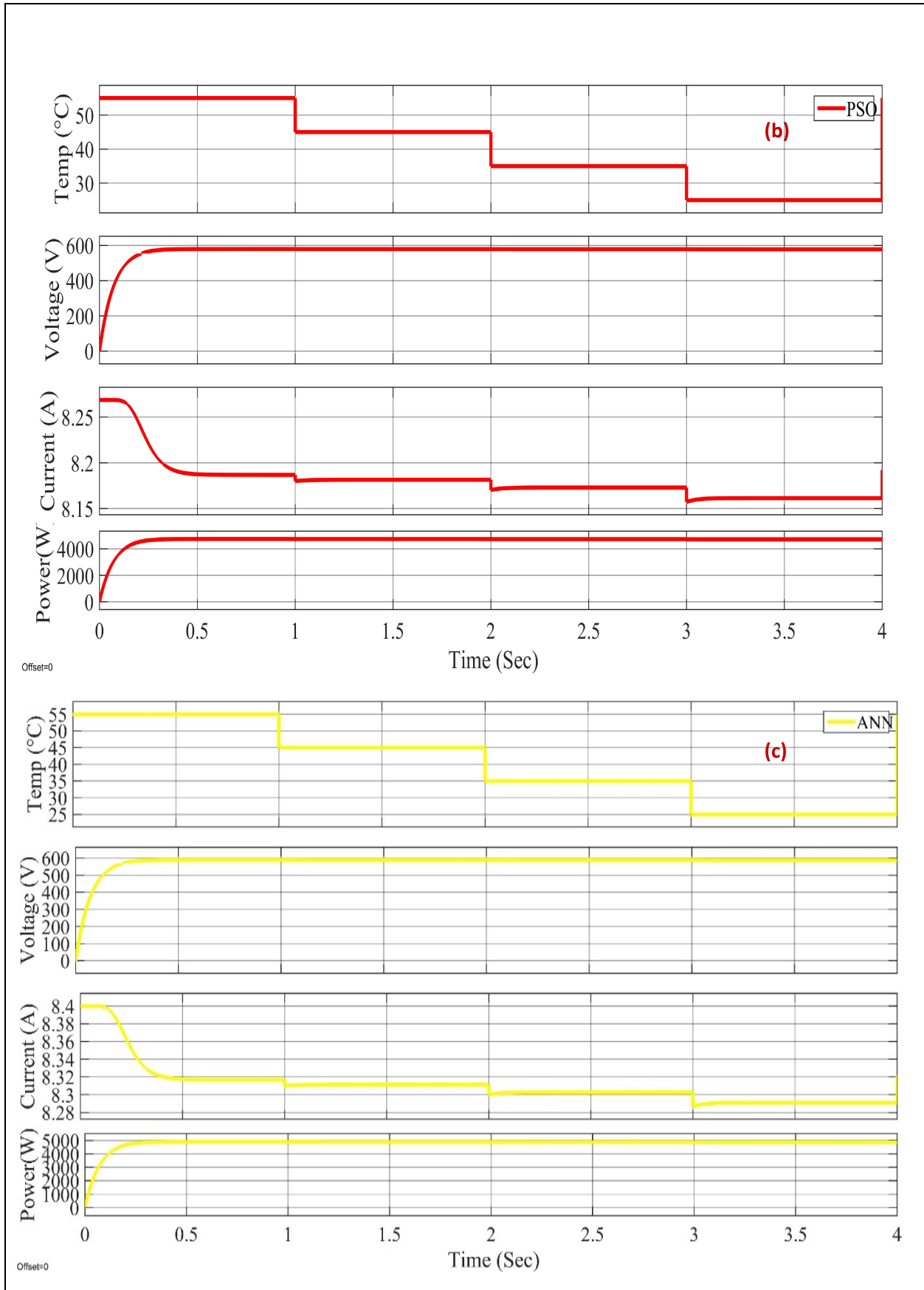
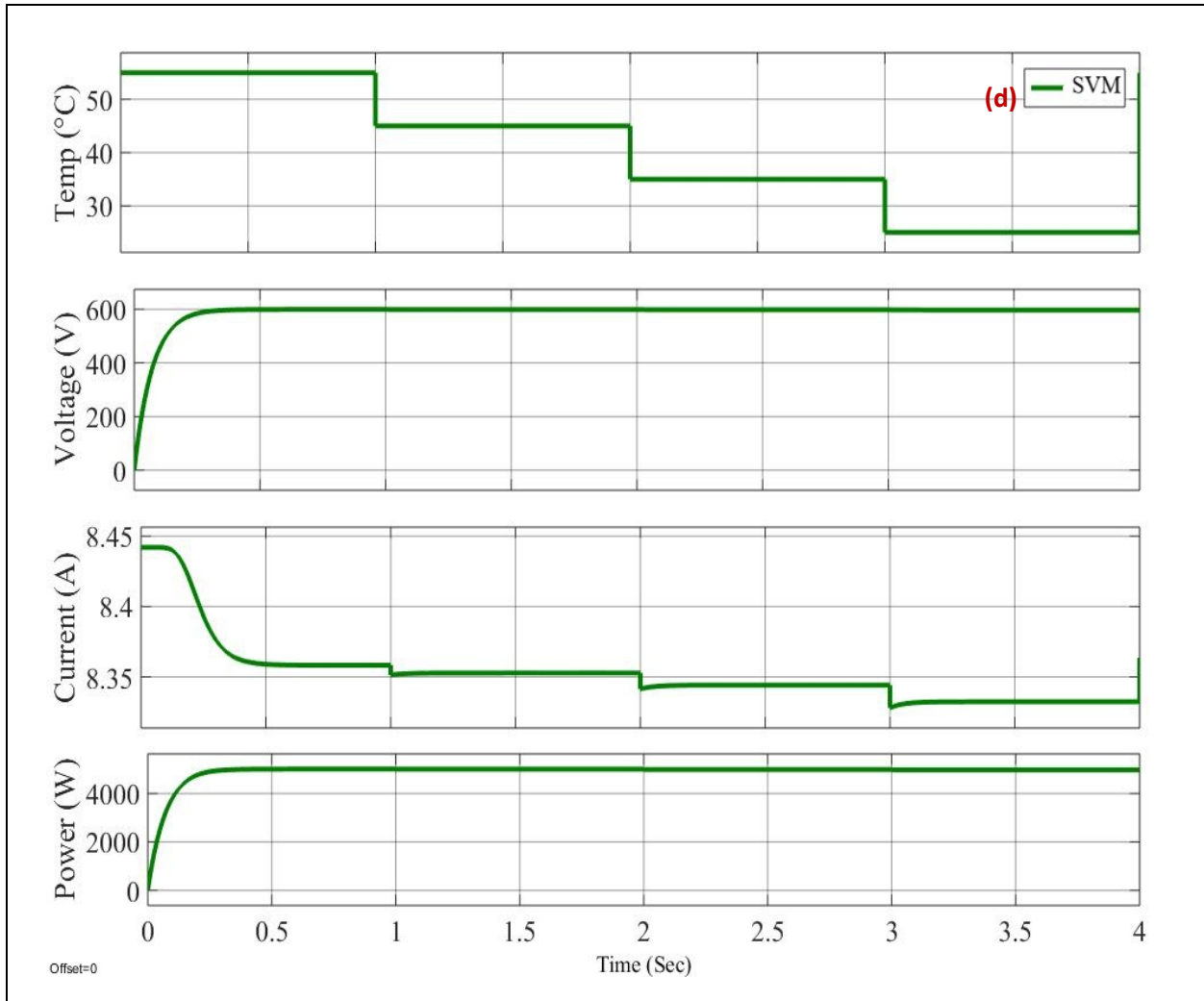


Fig. 6: PV generator current, voltage and power output at different solar irradiances







**Fig. 7: PV generator current, voltage and power output at different temperatures (a) Fuzzy (b) PSO (c) ANN and (d) ML**

Figure 6 shows the parameters of the solar PV generator, such as voltage ( $V_{pv}$ ), current ( $I_{pv}$ ), and power ( $P_{pv}$ ), under varying solar irradiation conditions ranging from 400 to 1000W/m<sup>2</sup>. At a solar irradiation of 400 W/m<sup>2</sup>, the values of voltage, current, and power are: 234.3V, 3.29A, and 770 watts for the fuzzy approach; 235.7V, 3.3A, and 777.8 watts for the PSO method; 239.5V, 3.36A, and 804.7 watts for the ANN method; and 243.5V, 3.37A, and 820.5 watts for the ML method. Similarly, the values of voltage, current, and power at irradiation of 1000 W/m<sup>2</sup> are 577.2V, 8.14A, and 4698 watts for the fuzzy approach, 580V, 8.18A, and 4744 watts for the PSO method, 589V, 8.3A, and 4888 watts for the ANN method, and 598V, 8.35A, and 4993 watts for the ML method. The data indicate that solar irradiation increases, and voltage, current, and power are also increasing. The overall efficiency of the PV solar power system increases with increasing irradiation.

Results of the solar PV generator  $V_{pv}$ ,  $I_{pv}$  and  $P_{pv}$  at different temperatures (25°C-55°C) are displayed

in Figure 7, with a constant insolation of 1000W/m<sup>2</sup>. Power and voltage decrease with increasing temperature. At a temperature of 25°C, the values of voltage, current, and power are: 577.2V, 8.11A, and 4681 watts for the fuzzy approach; 581V, 8.17A, and 4747 watts for the PSO method; 590V, 8.27A, and 4879 watts for the ANN method; and 600V, 8.33A, and 4998 watts for the ML method. Similarly, the values of voltage, current, and power at a temperature of 55°C are 574V, 8.14A, and 4672 watts for the fuzzy approach, 578V, 8.2A, and 4739 watts for the PSO method, 587V, 8.31A, and 4878 watts for the ANN method, and 596V, 8.36A, and 4982 watts for the ML method. The data indicate that temperature and current are increasing, but voltage and power are decreasing. As the short-circuit current increases, there is a more pronounced drop in cell voltage. The overall efficiency of the PV solar power system degrades with increasing temperature. In different weather conditions, ML technique-based systems perform better than the other techniques.

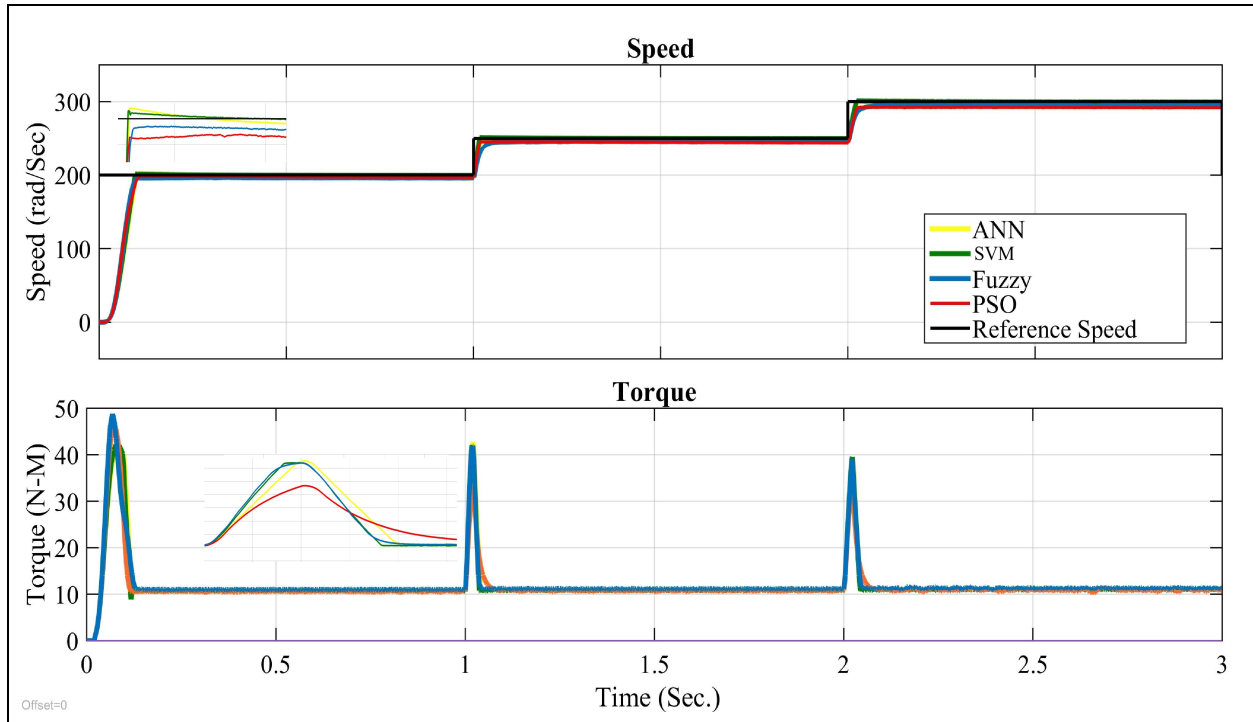


**Fig. 8: Speed and torque output at various speeds with constant torque**

Figure 8 shows the performance of the submersible motor pump speed at various speeds at constant load torque. At the start, the overshoot of ANN is high compared to ML. The settling time of ML is minimal compared to others. After 1 sec, the speed varies from 200 to 250 rad/sec; the conversion is smooth in ML compared to others. The starting torque overshoot in fuzzy is high. The settling time in PSO is high. The ML settlement time is minimal compared to others.

**Table 2. Compare different AI techniques based on speed, overshoot and settling time**

Techniques	Reference speed in rad/sec.			Overshoot (%)	Settling time (Sec.)
	200	250	300		
Fuzzy	196.5	244.8	292.3	-3	0.6
PSO	197.6	245.7	294.6	-2	0.55
ANN	198.5	248.6	298.4	2	0.5
ML	199.9	249.9	300	0.95	0.3

Table 2 shows the performance of various AI control methods at varying speeds, overshoot, and settling times. At reference speed 200, the average speed of Fuzzy, PSO, ANN and ML are 196.5 rad/sec, 197.6 rad/sec, 198.5 rad/sec and 199.9 rad/sec respectively. At reference speed 300, the average speed of Fuzzy, PSO, ANN and ML are 292.3 rad/sec, 294.6 rad/sec, 298.4 rad/sec and 300 rad/sec respectively. The results of the ML technique are consistently close to reference speed compared to other methods. Fuzzy techniques report an overshoot of -3% and a settling time of 0.6 seconds, PSO

strategies report an overshoot of -2% and a settling time of 0.55 seconds, ANN report an overshoot of -2% and a settling time of 0.5 seconds, while ML approaches report an overshoot of 0.95% and a settling time of 0.3 seconds. In terms of overshooting and settling time, ML gives better performance.

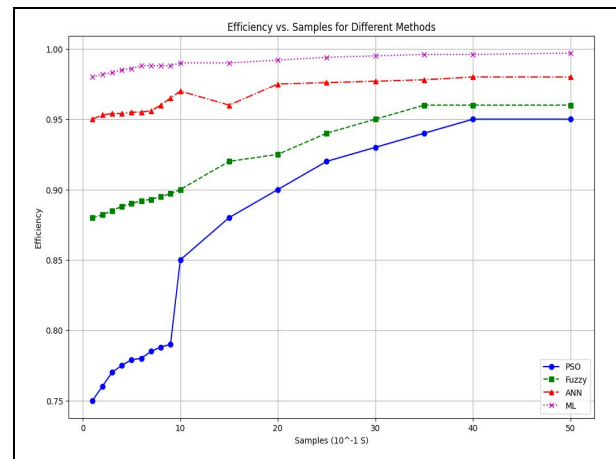


**Fig. 9: Comparison of system efficiency at different AI techniques**

Fig. 9 illustrates that PSO-based system efficiency is poor in starting samples. After 20 samples, it reaches 90% and constant 95% after 40 samples. Fuzzy-based system efficiency is good compared to PSO and less than ANN and ML. The performance of ANN techniques is better than that of PSO and fuzzy. The ML-based system is constantly maintained and has reached

99.6%. It is clear from the graph; ML technique performance is better than the others.

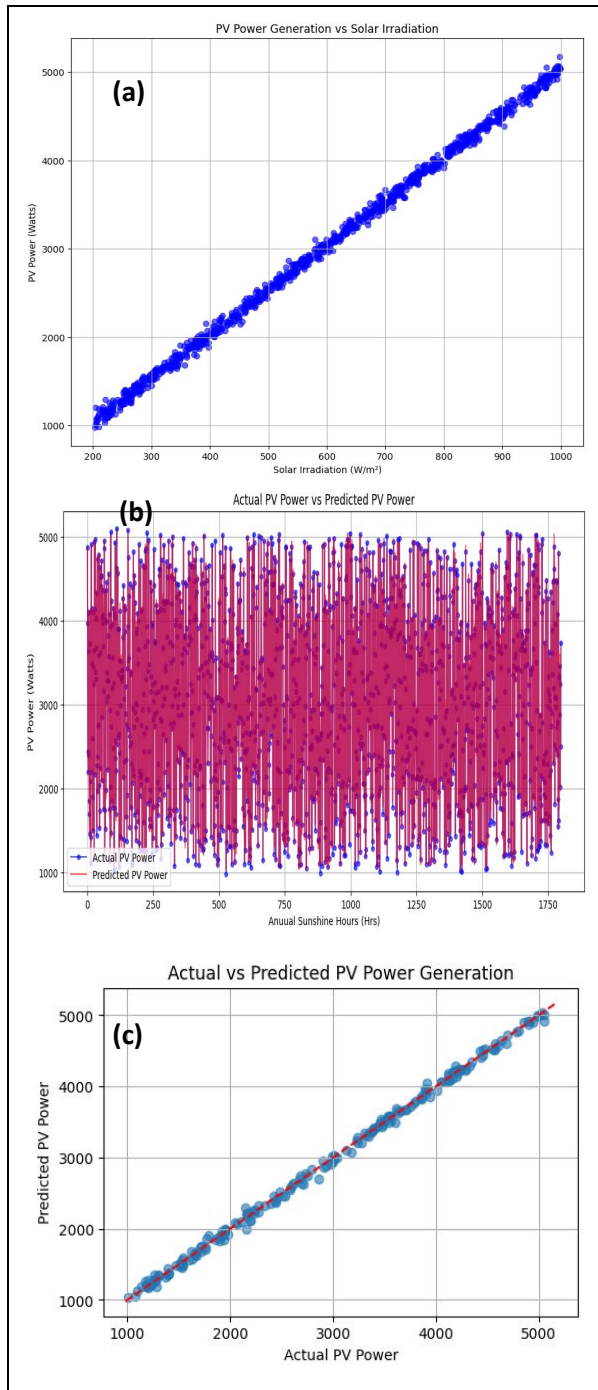


**Fig. 10. SV-ML optimization results (a) Comparison of generated PV power at different solar irradiation, (b) Annual actual and predicted PV power generation at sunshine hours and (c) Comparison of actual PV power and predicted PV power**

Figure 10a shows the generation of ML (SVM) based PV power at different levels of sun irradiation. Increased irradiation results in an increase in PV power. Solar irradiation of  $1000\text{W}/\text{m}^2$  allowed the PV module to

reach its maximum capacity. The use of ML algorithms yields results that are more accurate when applied to real-time data.

Figure 10b illustrates the annual PV power generated during sunlight hours. ML (SVM) is utilized to forecast PV power. The generation of PV power is evaluated from 10:00 AM to 3:00 PM. The results indicate that the ML algorithms accurately estimate the generated power. Figure 10c illustrates the comparison between real PV power and predicted PV output. The expected power is closely aligned with the actual power.

## 6. CONCLUSION

A 5-kW PV solar-powered irrigation system was constructed according to daily water requirements. PV system performance was evaluated under varying sun irradiance and temperature conditions. PSO, ANN, fuzzy logic, and ML techniques have been employed for optimization. This study also examined the efficiency and prediction of PV-generated power. The case study load demand is 30,000 litres/day. The components of the PV system have been determined: the inverter is rated at 4 kW, the DC-DC converter at 4.5 kW, and the PV capacity at 5 kW. The PV system is evaluated under different solar irradiance conditions ( $300\text{W}/\text{m}^2$  to  $1000\text{W}/\text{m}^2$ ) and temperature conditions ( $25^\circ\text{C}$  to  $55^\circ\text{C}$ ). The AI techniques (fuzzy logic, PSO, ANN, and ML) have been developed and implemented in MPPT as a control mechanism. The performance of the MPPT-based system has been evaluated in different weather situations. The values of voltage, current, and power at irradiation of  $1000\text{W}/\text{m}^2$  are 577.2V, 8.14A, and 4698 watts for the fuzzy approach, 580V, 8.18A, and 4744 watts for the PSO method, 589V, 8.3A, and 4888 watts for the ANN method, and 598V, 8.35A, and 4993 watts for the ML method. At a temperature of  $25^\circ\text{C}$ , the values of voltage, current, and power are: 577.2V, 8.11A, and 4681 watts for the fuzzy approach; 581V, 8.17A, and 4747 watts for the PSO method; 590V, 8.27A, and 4879 watts for the ANN method; and 600V, 8.33A, and 4998 watts for the ML method. Under varying weather conditions, systems based on ML technique exhibit superior performance compared to PSO, fuzzy and ANN methods.

To optimize the analysis of motor pump performance at varying speeds (200-300 rad/sec). Table 2 illustrates the performance of AI control methods at different speeds, overshoots, and settling times. At a reference speed of 300, the average speeds of Fuzzy, PSO, ANN, and ML are 292.3 rad/sec, 294.6 rad/sec, 298.4 rad/sec, and 300 rad/sec, respectively. The ML technique consistently aligns with the reference speed. The ML technique also reduces the overshoot and the settling time. The efficiencies are as follows: PSO (95%), fuzzy logic (96%), ANN (98%), and ML (99.6%). The comparative results indicate that the ML (SVM) technique is superior and more efficient than others. ML

(SVM) also predicts the generation of electricity from PV power. The findings demonstrate that the ML (SVM) algorithms effectively predict the generated power. The research work is to improve quality of life and promote an environmentally sustainable atmosphere in remote areas by implementing a more stable, efficient, and effective solar powered irrigation system utilising AI techniques.

## FUNDING

This research received no specific grant from any funding agency in the public, commercial, or not-for-profit sectors.

## CONFLICTS OF INTEREST

The authors declare that there is no conflict of interest.

## COPYRIGHT

This article is an open-access article distributed under the terms and conditions of the Creative Commons Attribution (CC BY) license (<http://creativecommons.org/licenses/by/4.0/>).



## REFERENCES

- Abid, M. Z., Muhammad, Y., Saleem, U. and Muhammad, Hassan., Design, Sizing and Economic Feasibility of a Hybrid PV/Diesel/Battery Based Water Pumping System for Farmland, *Int. J. Green Energy*, 19(6), 614–37(2022). <https://doi.org/10.1080/15435075.2021.1954007>
- Agarwal, A., Kumar, N. and Dubey, P., Machine Learning Based Maximum Power Prediction for Photovoltaic System, *Indian J. Pure Appl. Phys.*, 60 (10), 892–898(2022). <https://doi.org/10.56042/ijpap.v60i10.62197>
- Ahmad, K.R., Farrukh, S., Logavani, K., Catherine, T. J., Shimpy, R., Singh, M., Prabu, R. T., Bala, B. S. and Adane, K., Maximum Power Point Tracking of PV Grids Using Deep Learning, *Int. J. Photoenergy*, 2022(1), 1123251(2022). <https://doi.org/10.1155/2022/1123251>
- Bacanin, N., Luka, J., Zivkovic, M., Kandasamy, V., Milos, A., Deveci, M. and Ivana, S., Multivariate Energy Forecasting via Metaheuristic Tuned Long-Short Term Memory and Gated Recurrent Unit Neural Networks, *Inf. Sci.*, 642, 119122(2023). <https://doi.org/10.1016/j.ins.2023.119122>
- Bandhu, K. C., Litoriya, R., Khatri, M., Milind, K. and Prakhar, S., A Novel Approach for Better Career Counselling Utilizing Machine Learning Techniques, *Wireless Pers. Commun.*, 138, 2523-2560(2024). <https://doi.org/10.1007/s11277-024-11612-3>
- Deo, R. C., X. Wen, and F. Qi., A Wavelet-Coupled Support Vector Machine Model for Forecasting Global Incident Solar Radiation Using Limited Meteorological Dataset, *Appl. Energy*, 168, 568–593(2016). <https://doi.org/10.1016/j.apenergy.2016.01.130>
- Der, L. S., Liu, H. D., Wang, M. H. and Wu, C. C., A Novel Strategy for Multitype Fault Diagnosis in Photovoltaic Systems Using Multiple Regression Analysis and Support Vector Machines, *Energy Rep.*, 12, 2824–2844(2024). <https://doi.org/10.1016/j.egyr.2024.08.074>
- Gupta, M. and Bhargava, A., Optimal Design of Hybrid Renewable-Energy Microgrid System: A Techno-Economic–Environment–Social–Reliability Perspective, *Energy Rep.*, 8(1), 66–83(2024). <https://doi.org/10.1093/ce/zkad069>
- Habib, S., Liu, H., Tamoor, M., Hussien, A. G., Zawbaa, H. M. and Salah, K., Technical Modelling of Solar Photovoltaic Water Pumping System and Evaluation of System Performance and Their Socio-Economic Impact, *Heliyon*, 9(5), e16105(2023). <https://doi.org/10.1016/j.heliyon.2023.e16105>
- Hafdaoui, H., Kouadri, B. E. A., Chahtou, A., Bouchakour, S. and Belhaouas, N., Analyzing the Performance of Photovoltaic Systems Using Support Vector Machine Classifier, *Sustainable Energy Grids Net.*, 29, 100592(2022). <https://doi.org/10.1016/j.segan.2021.100592>
- Jayasankar, K. C., Anandhakumar, G. and Kalaimurugan, A., Fuzzy Logic Controller-Based Intelligent Irrigation System Using Solar Radiation Data, *J. Environ. Nanotechnol.*, 13(2), 37–45(2024). <https://doi.org/10.13074/jent.2024.06.242586>
- Khan, K., Rashid, S., Mansoor, M., Khan, A., Hasan, R., Zafar, H. M. Akhtar, N. and Raza, H., Data-driven Green Energy Extraction: Machine Learning-Based MPPT Control with Efficient Fault Detection Method for the Hybrid PV-TEG System, *Energy Rep.*, 9, 3604–3623(2023). <https://doi.org/10.1016/j.egyr.2023.02.047>
- Khasawneh, H. J., Zaid, A. G., Waseem, M. A. K., Ahmad, M. A. H. and Zaid, M. A., Creating Optimized Machine Learning Pipelines for PV Power Generation Forecasting Using the Grid Search and Tree-Based Pipeline Optimization Tool, *Cogent Eng.*, 11(1), 2323818(2024). <https://doi.org/10.1080/23311916.2024.2323818>
- Kirubakaran, S. V. and Singaravelu, S., Enhancing Solar Photovoltaic Systems through Advanced MPPT Control: A Comparative Analysis of AI-Based Techniques and a Novel ML-Based SVR Model for Optimal Performance and Stability, *SSRG Int. J. Electron. Commun. Eng.*, 11(1), 39–52(2024). <https://doi.org/10.14445/23488549/IJECE-V11I1P104>

- Koç, C., A study on operation problems of hydropower plants integrated with irrigation schemes operated in Turkey, *Int. J. Green Energy*, 15(2), 129–135(2018). <https://doi.org/10.1080/15435075.2018.1427591>
- Li, J., Herdem, M. S., Nathwani, J. and Wen, J. Z., Methods and Applications for Artificial Intelligence, Big Data, Internet of Things, and Blockchain in Smart Energy Management, *Energy AI*, 11, 100208(2023). <https://doi.org/10.1016/j.egyai.2022.100208>
- Liu, W., Shen, Y., Aungkulanon, P., Binh, L. N., Meza, A. A., Yulineth, C. E. and Ghalandari, M., 2023. Machine Learning Applications for Photovoltaic System Optimization in Zero Green Energy Buildings, *Energy Rep.*, 9, 2787–2796(2023). <https://doi.org/10.1016/j.egy.2023.01.114>
- Mahesh, P. V., Meyyappan, S and Alla, R. R., Maximum Power Point Tracking Using Decision-Tree Machine-Learning Algorithm for Photovoltaic Systems, *Clean Energy*, 6(5), 762–775(2022a). <https://doi.org/10.1093/ce/zkac057>
- Mahesh, P. V., Meyyappan, S. and Alla, R. R., Maximum Power Point Tracking with Regression Machine Learning Algorithms for Solar PV Systems, *Int. J. Renewable Energy Res.*, 12(3), 1327–1338(2022b). <https://doi.org/10.20508/ijrer.v12i3.13249.g8517>
- Meena, R. S., Anoop, S., Shilpa, U., Rohit, B., Neeraj, K. G., Israr, M., Kothari, D. P., Chiranjeevi, C. and Prasath, S., Artificial Intelligence-Based Deep Learning Model for the Performance Enhancement of Photovoltaic Panels in Solar Energy Systems, *Int. J. Photoenergy*, 2022(1), 3437364(2022). <https://doi.org/10.1155/2022/3437364>
- Mohammad, A. and Mahjabeen, F., Revolutionizing Solar Energy with AI-Driven Enhancements in Photovoltaic Technology, *J. Multidiscip. Sci.*, 2(4), 1174–1187(2023).
- Omer, Z. M., and Shareef, H., An Adjustable Machine Learning Gradient Boosting-Based Controller for PV Applications, *Intell. Syst. Appl.*, 19, 200261(2023). <https://doi.org/10.1016/j.iswa.2023.200261>
- Ourici, A. and Abderaouf, B., Maximum Power Point Tracking in a Photovoltaic System Based on Artificial Neurons, *Indian J. Sci. Technol.*, 16(23), 1760–1767(2023). <https://doi.org/10.17485/ijst/v16i23.648>
- Pan, M., Chao, L., Ran, G., Huang, Y., You, H., Tangsheng, G. and Qin, F., Photovoltaic Power Forecasting Based on a Support Vector Machine with Improved Ant Colony Optimization, *J. Cleaner Prod.*, 277, 123948(2020). <https://doi.org/10.1016/j.jclepro.2020.123948>
- Pandey, M., Litoriya, R. and Pandey, P., Analyzing Student Dropout Factors in Engineering Courses Using a Fuzzy Based Decision Support System, *Multimedia Tools Appl.*, 83, 87045-87069(2024). <https://doi.org/10.1007/s11042-024-19810-8>
- Pandian, P. S., Gnanapoo, T., Denosha, R., Kumar, S. R., and Sivaiah, B. V., Real-Time Fault Detection in Solar PV Systems Using Hybrid ANN – SVM Machine Learning Algorithm, *Int. J. Intel. Syst. Appl. Eng.*, 12(22), 1367-1374(2024).
- Raghuwanshi, S. S., and Khare, V., Sizing and Modelling of Stand-Alone Photovoltaic Water Pumping System for Irrigation, *Energy Environ.*, 29(4), 473-491(2018). <https://doi.org/10.1177/0958305X17752739>
- Raghuwanshi, S. S., Raghuwanshi, P., Masih, A. and Singh, P., Modeling and Optimization of Hybrid Renewable Energy with Storage System Using Flamingo Swarm Intelligence Algorithms, *Energy Storage*, 5(7), e470(2023). <https://doi.org/10.1002/est2.470>
- Raj, V., Dotse, S. Q., Sathyajith, M., Petra, M. I. and Yassin, H., Ensemble Machine Learning for Predicting the Power Output from Different Solar Photovoltaic Systems, *Energies*, 16(2), 671(2023). <https://doi.org/10.3390/en16020671>
- Sharmin, R., Chowdhury, S. S., Abedin, F. and Rahman, K. M., Implementation of an MPPT Technique of a Solar Module with Supervised Machine Learning, *Front. Energy Res.*, 10, 2296-5980(2022). <https://doi.org/10.3389/fenrg.2022.932653>
- Shah, H., Nilesh, G. C. and Jaydeep, C., AI-Based Fault Recognition and Classification in the IEEE 9-Bus System Interconnected to PV Systems, *Smart Sci.*, 12(1), 185–197(2024). <https://doi.org/10.1080/23080477.2023.2285275>
- Sinha, M. K., Piyush, C., Shrunkhala, S., Halve, P. M. and Santosh, S. R., Design and Optimization of Hybrid Solar PV Energy System for Rural Areas in the Narmada Valley, India, *Int. J. Ambient Energy*, 45(1), 2402773(2024). <https://doi.org/10.1080/01430750.2024.2402773>
- Verma, R., Bhatia, R. and Raghuwanshi, S. S., Optimization and Performance Enhancement of Renewable Energy Microgrid Energy System Using Pheasant Bird Optimization Algorithm, *Sustainable Energy Technol. Assess.*, 66, 103801(2024). <https://doi.org/10.1016/j.seta.2024.103801>
- Venkat, R. A., Suresh, B. G. and Satish, K. P., Islanded Micro-Grid under Variable Load Conditions for Local Distribution Network Using Artificial Neural Network, *Smart Sci.*, 12(4), 622-637(2024). <https://doi.org/10.1080/23080477.2024.2358672>